

# CONVEYANCE ROLLER NIP MECHANICS

BY

KEVIN COLE, PhD

Senior Web Handling Development Engineer

Optimation Technology Incorporated

## Introduction

Nip rollers are used extensively in converting processes; however, elastomeric-covered rollers have the unwanted and often unpredictable characteristic of unknown surface speed owing to coupling between circumferential and radial strains within the nip. Variations in nip roller feed rate due to width-dependent effects such as roller deflection can lead to web troughing and wrinkling propensity.

In this paper, we review measurement methods for accurately measuring nip roller feed rates. Modeling techniques are presented for predicting width-dependent nip roller feed rates due to roller loading and width-dependent bending. Discussion regarding the practical implications of the width-dependent behavior is given. Experimental data from the Optimation Technology Media Conveyance Facility for all aspects of this work will also be presented.

This paper, while providing theoretical and experimental details on nip mechanics, will also serve as a useful tutorial for those interested in learning about the practical operational aspects of nip rollers.

## Nip Mechanics Overview

When webs are conveyed by elastomeric-covered nip rollers, it is often the case that the speed of the web is different from the nominal surface speed of the rollers away from the nip (see Stack et. al. [1995]). This behavior is influenced by a number of factors, including the physical properties of the elastomeric coverings, geometric characteristics such as cover thicknesses and roller diameters and process conditions such as the engagement of the rollers and tension difference in the web across the nip rollers. Owing to this behavior, nip systems are often comprised of one elastomeric covered roller and one roller without an elastomeric covering. The web is typically wrapped over the uncovered roller and if the nip roller pair is a drive, the uncovered roller is usually driven. This being said, deleterious effects due to the inherent tendency of the elastomeric-covered roller to travel at a different nominal surface speed compared to the web speed can still be present. Two examples are: (a) small relative motion (e.g., micro-creep) in the machine direction leading to the potential for abrasions and dirt generation and (b) differential relative motion in the transverse direction leading to an increased risk of the formation of unwanted lateral tracking and wrinkling. Transverse direction effects can arise due to differing amounts of roller engagement due to roller core bending effects. This follows from the fact that the differential surface speed is a function of roller engagement.

Figure 1 shows a cross sectional view of an elastomeric roller (number 1) loaded against an uncovered backing roller (number 2). No web is considered to be in the system. Prior to contact,

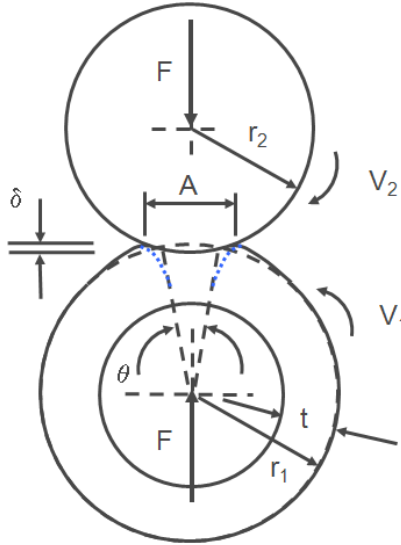


Figure 1: Nip roller system cross-sectional view

each particle on the surface of each roller rotates at the same surface speed,  $V$ . Assuming roller 2 to be driven, it will still travel at the same surface speed after the rollers are brought into engagement by an amount,  $\delta$ . Therefore,  $V_2 = V$ . However,  $V_1$  will no longer be equal to  $V$ . To determine  $V_1$ , it is noted that the characteristics of the elastomeric covering on roller 1 determine the circumferential strain that develops within the contact, or nip, zone. The angle,  $\theta$ , is defined as the angle subtended by the nip zone in roller 1 assuming that there is no circumferential strain in the cover. Under this assumption, the nip width is equal to  $r_1\theta$  and the interval of time,  $\Delta t$ , required for roller 1 to rotate through this angle is found from the following:

$$\Delta t = r_1\theta / V_1 \quad (1)$$

Owing to the coupling between radial and circumferential strains, the actual nip width,  $A$ , will be different than the theoretical nip width by some nominal amount,  $\epsilon$ , which we refer to as the creep of the system:

$$A = (1 + \epsilon)r_1\theta \quad (2)$$

The creep is the average circumferential strain in the nip zone which, as we shall next show, relates to the speed of roller 1. Owing to mass conservation, a particle on the surface of roller 2 must travel through the actual nip in the same interval of time as roller 1 rotates through  $\theta$ .

$$\Delta t = A / V_2 = A / V \quad (3)$$

Combining equations (1) through (3) yields the surface velocity of roller 1 in terms of the creep:

$$V_1 = V / (1 + \varepsilon) \quad (4)$$

Equation (4) indicates that for positive creep, the elastomeric-covered roller will travel at a slower speed than the drive roller and that for negative creep, the elastomeric-covered roller will travel at a higher speed than the drive roller.

For linear elastic materials, there are two material constitutive properties that influence the relationships between deflections, loads and creep within a system such as shown in Figure 1. The first, Young's modulus,  $E$ , is roughly a measure of radial stiffness and the second, Poisson's ratio,  $\nu$ , is a measure of compressibility.

Reference 2 (Good [2001]) provides detailed information about both of these properties. In that work, it was shown that for natural and synthetic rubbers, Shore A (i.e., IRHD) hardness measured with a hand-held instrument is adequate to predict Young's modulus. The relationship between Shore A hardness and modulus was found to be given by the following expression (reference 2, equation 1):

$$E_o = 20.97e^{0.0564*IRHD} \text{ (psi)} \quad (5)$$

where the subscript indicates modulus excluding confinement effects. Suitable modifications to account for confinement in the nip zone are provided (reference 2, equation 5).

For linear elastic materials, a value of Poisson's ratio approaching 0.5 corresponds to an incompressible material. Materials such as polyurethanes and rubbers have a Poisson's ratio approaching 0.5. Owing to the incompressible nature of these types of typical roller coverings, radial strains due to roller engagement leads to significant positive circumferential strain resulting in positive values of creep. Reference 2 reports that a value of 0.46 seems to be valid over a wide range of durometers and elastomeric materials. We will use this value in the work that follows.

At the other extreme, open cell foams have a Poisson's ratio approaching 0. In this case, creep may actually be negative resulting in a roller covered with such a material going faster than the driven roller. One such case will be examined in the work that follows.

### Nip Deflection/Nip Roller Feed Rate Models

Reference 2 (Good [2001]) provides a description of several nip deflection models relating nip width to roller engagement or deflection. The most useful of these models is that proposed by Johnson (reference 2, equation 18):

$$F = \frac{2(1-\nu)^2}{3} \frac{E_0}{1-2\nu} \frac{\sqrt{2R}}{1-\nu^2} \frac{\delta^{3/2}}{t} \quad (6)$$

where  $\nu$  is Poisson's ratio,  $R$  is the equivalent radius (which for a pair of rollers shown in Figure 1 can be written as  $R=(R_1R_2)/(R_1+R_2)$ ),  $t$  is the cover thickness on roller 1, and  $\delta$  is the engagement of the two rollers. A corrected version of equation 6 accounting for rubber confinement in the nip zone is provided by equation 27 in reference 2.

Unfortunately, the model provided by equation (6) does not predict creep. For that purpose, we describe two additional models. The first, referred to as the "Approximate" creep model, makes simplifying assumptions about the behavior in the nip to develop predictions of creep along with load/deflection and nip width/load and is presented next. This model, somewhat heuristic, provides us with an ability to develop an understanding of how the geometric and material properties of the system affect the creep performance. The second, referred to as the "Cole" model, predicts the same responses more accurately since it is developed from first principles. The load/deflection results from these two models will be compared to equation (6) and the creep predictions will be compared to experimental data collected using a method that is described in the next section. This model has been described elsewhere (reference 3, Cole [2010]) and so is only briefly discussed here.

For the Approximate creep model (reference 4, Cole [1983]), the creep is approximated by:

$$\varepsilon = \alpha_1 \frac{2}{3} \frac{\delta}{t} \quad (6a)$$

where  $\alpha_i$  is a proportionality constant relating the actual creep to the average radial strain ( $\delta/t$ ) based on the assumption that the deflection follows a parabolic distribution within the nip. The deflection is also found from an approximate model that expresses, to within an adjustable constant, the geometric relationship between deflection and nip width:

$$\delta = \frac{A^2}{8\beta R} \quad (6b)$$

The constant  $\beta$  accounts for circumferential squeezing out of rubber that tends to increase the nip width for a given deflection. This effect is dependent on the ratio of cover thickness to roller radius as well as material properties. This parameter exceeds one as this ratio decreases. However, for the rollers studied in this report, a reasonable range of  $\beta$  is found to be between 0.65 and 1. This is confirmed with experimental measurements described in the next section where a value of  $\alpha_i$  is found to be approximately 0.50. Combining equations 6a and 6b yield the following simplified result for creep in terms of the variables of the analysis:

$$\varepsilon = \alpha_1 \frac{2}{3} \frac{A^2}{8\beta R t} \quad (6c)$$

From references 5 (Hannah [1951]) and 6 (Parish [1961]), we find the following approximate solution for nip width in terms of nip load:

$$A = 4 \sqrt{\frac{FR(1-\nu^2)}{\pi E}} \left\{ 1 - \frac{.35}{t} \sqrt{\frac{FR(1-\nu^2)}{\pi E}} \right\} \quad (6d)$$

where  $F$  is the nip loading per unit length. Finally, we substitute equation (6d) into (6b) and (6c) to give deflection and creep as a function of nip load, cover thickness, and cover properties:

$$\delta = \frac{2F(1-\nu^2)}{\pi E \beta} \left\{ 1 - \frac{.35}{t} \sqrt{\frac{FR(1-\nu^2)}{\pi E}} \right\}^2 \quad (6e)$$

$$\varepsilon = \alpha_1 \frac{4}{3} \frac{F(1-\nu^2)}{\pi E \beta t} \left\{ 1 - \frac{.35}{t} \sqrt{\frac{FR(1-\nu^2)}{\pi E}} \right\}^2 \quad (6f)$$

Equations (6e) and (6f) are valid for the cases where either one roller is hard and the other has a covering or both rollers are symmetrical with each having the same cover thickness. Observation of equation (6f) indicates that to first order, creep is proportional to load and inversely proportional to material modulus and cover thickness. In addition, the model indicates that creep is a weak inverse function of equivalent radius. These trends are supported by the more exact model to be described next. However, the Approximate model would also indicate that increasing Poisson's ratio would lead to a decreasing amount of creep. This is incorrect owing to the fact that the creep constant,  $\alpha_i$ , increases with increasing Poisson's ratio.

A very brief overview of the Cole model is now be provided. Reference 7 (Timoshenko [1970]) also provides a discussion of this solution method. The model first develops closed form analytical solutions to the problem of stresses and strains within a finite thickness layer(s) of linear elastic material. The solutions are exact assuming sinusoidal loading and displacements.

Fourier series expansion is then used to solve for the response at one point along the surface of the strip due to a load at another point. To facilitate the derivation, the interpolation function,  $sinc(x)=sin(x)/x$ , where  $x$  is the coordinate along the length of the strip. This function has the desirable characteristic of equaling 1 at the load application point and zero at all other equally spaced points away from the load point. The response of the strip to this interpolation function can be found by means of a Fourier integral over a finite frequency range since the *Sinc* function has the further desirable characteristic of having a finite frequency spectrum.

Application of the general strip solution to the nip roller pair shown in Figure 1 is made by writing geometric compatibility equations accounting for the cylindrical geometry of the rollers. For a specified roller engagement, the displacement within the nip is known and outside of the nip, the normal stress is equal to zero. The nip width, initially unknown, is found by iteration until the boundary conditions inside and outside of the nip zone are satisfied. Once a solution is found, the circumferential creep is computed by averaging the lengthwise strains in the nip zone.

Figures 4 through 6 show a comparison of results from the KL Johnson model (equation 6), the Approximate model, the Cole model and experimental data obtained from the Thin Web Rewinder (TWR) in the Optimization Media Conveyance Facility. In the next section, the method used to obtain the experimental results will be described. The results are for a nip roller pair with the following characteristics (refer to Figure 1 for geometry): roller #1 radius = 3.005 inch, elastomeric cover thickness (one layer) = 0.375 inch, elastomer cover durometer = 50 Shore A, elastomer cover Poisson's ratio = 0.46, and roller #2 radius = 6.3095 inch.

Figure 4 shows nip load versus deflection and indicates good agreement between the three models. The measured data, however, does not agree well with the theoretical data. The reason for the discrepancy was determined to be due to the fact that the deflection was measured at the

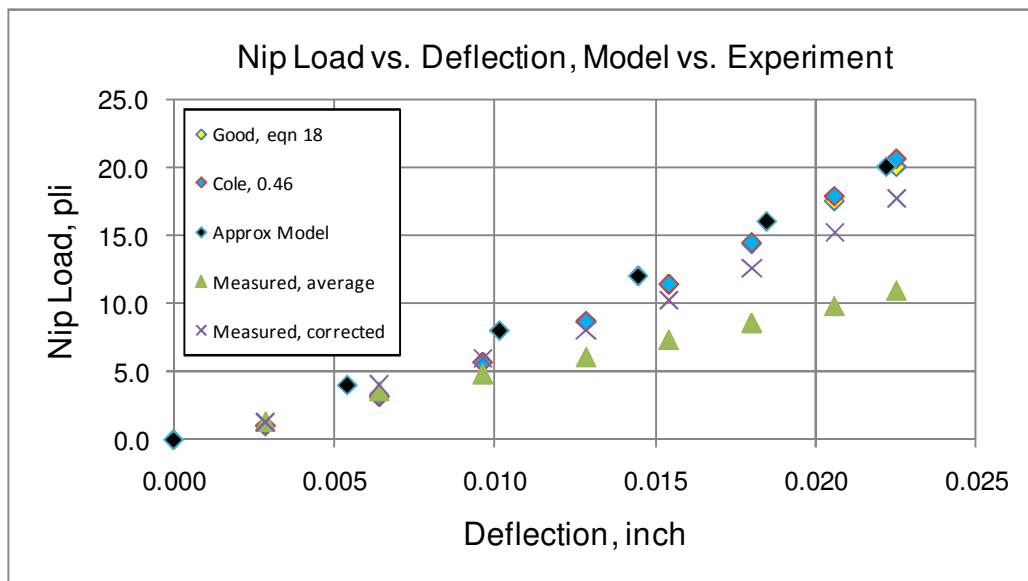


Figure 4: Nip Load versus Roller Deflection, baseline case

end of the roller where the nip load was greater than the nominal nip load across the width of the roller. Correcting for this difference yielded results in better agreement with theory.

Figure 5 is a graph of nip width versus nip load. Again, excellent agreement is seen between theory's and the measured nip width versus nip load. The measured values are the average over four measurements across the width of the roller.

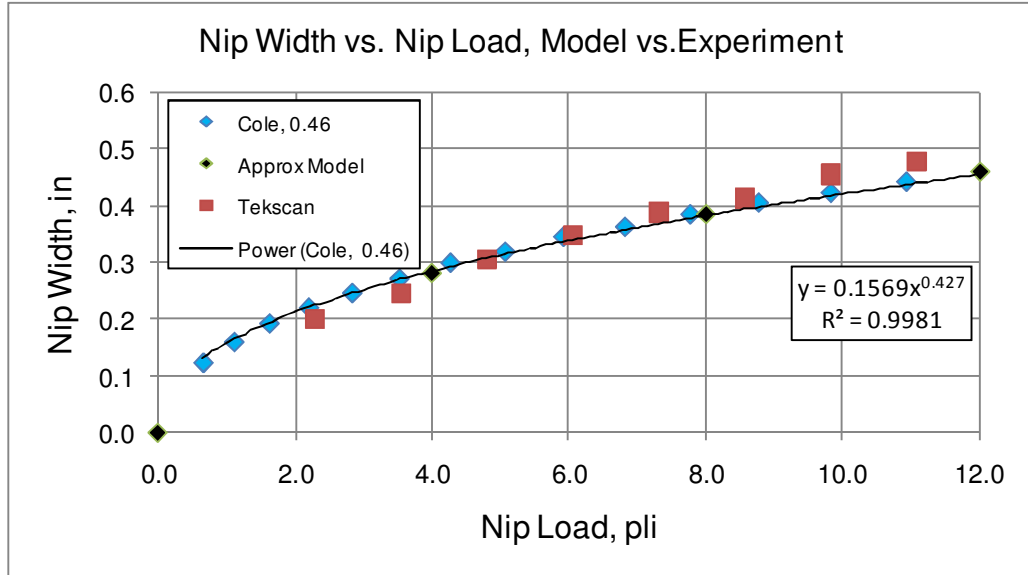


Figure 5: Nip Width versus Nip Load, baseline case

Creep is plotted in Figure 6. For positive creep, the elastomeric covered roller rotates at a reduced speed. This result is expected for a single layer of very nearly incompressible material. The agreement between theory and experiment is not as good as the previous predictions and perhaps reflects the effect of neglecting friction in the nip zone. However, small changes in Poisson's ratio near 0.5 will have a rather large effect on predictions of creep. The curve for

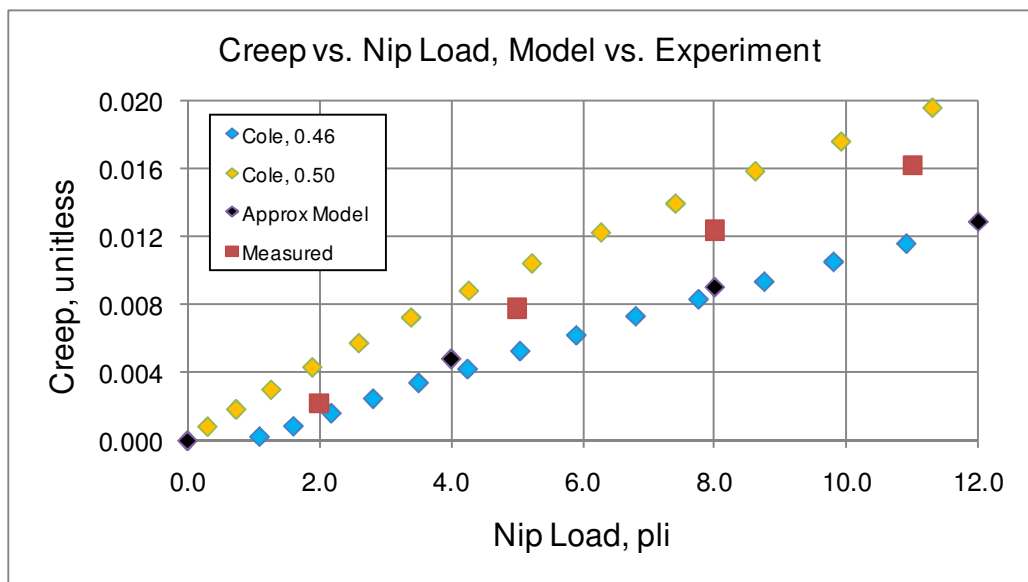


Figure 6: Creep versus Nip Load, baseline case

Poisson's ratio equals to 0.5 is also shown in Figure 6 and the agreement between experiment and prediction would appear to be best at some intermediate value of Poisson's ratio.

So which value of Poisson's ratio should be used? Based on the overall agreement between the experimental data, the value of 0.46 gives the best overall agreement between load/deflection and nip width/nip load while the value of 0.48 gives the best agreement between creep/nip load. Owing to the assumptions used to compute creep (no friction, average of the strain within the nip zone), it is believed that a stronger weighting needs to be given to the load/deflection/nip width data. Therefore, 0.46 is used in the results which follow (as per reference 2).

### Measurement of Load/Deflection and Creep

Experiments were conducted in the Media Conveyance Facility to obtain experimental data to verify the models described in the previous section. For this purpose, a nip roller module duplicating the configuration shown in Figure 1 was constructed on the TWR. A picture of the module is shown in Figure 7. The configuration consists of an idling lower uncovered roller and an upper roller with an elastomeric covering. Both are driven at a constant machine speed by means of a 12 micron PET web wrapped partially around the lower uncovered roller. Nip force is controlled by two air cylinders mounted at either end of the live-shafted elastomeric covered



Figure 7: Nip module setup on TWR

nip roller. The nip roller is attached to two pivoting arms which maintain alignment and provide a reference to measure roller engagement using mechanical dial indicators.

Nip width is measured using the Tekscan™ I-Scan measurement system. This system consists of sensors that detect pressure changes as an electrical resistance drop through a conductive ink. In

the results presented in the previous section, the nip width was measured at 4 locations across the width of the roller and averaged to give the results shown in Figure 5.

Creep was measured using a “*spindown tester*”. A spindown tester is an electronic instrument intended for accurately measuring the angular velocity and angular acceleration of a roller. Its operation is described in detail in reference 3. From this measurement, the time per roller rotation is computed to an accuracy of about 0.4 microseconds.

Creep can be computed from a knowledge of the rotation times for the two rollers according to the following equations:

$$t_1 = 2\pi(1 + \varepsilon)r_1/V \quad (7)$$

and

$$t_2 = 2\pi r_2/V \quad (8)$$

giving:

$$\varepsilon = r_2 t_1 / r_1 t_2 - 1 \quad (9)$$

### Measurement of Dual Durometer Roller Creep

Two additional rollers, provided by American Roller Company, were tested to assess the creep prediction theory. One roller was constructed with a single elastomeric layer ( $r_l = 3.125$  inch,  $t = 0.500$  inch, durometer = 40 Shore A, Poisson’s ratio assumed equal to 0.46) and the second was constructed with a dual layer ( $r_l = 3.3125$  inch,  $t_{inner} = 0.690$  inch,  $t_{outer} = 0.060$  inch, inner layer

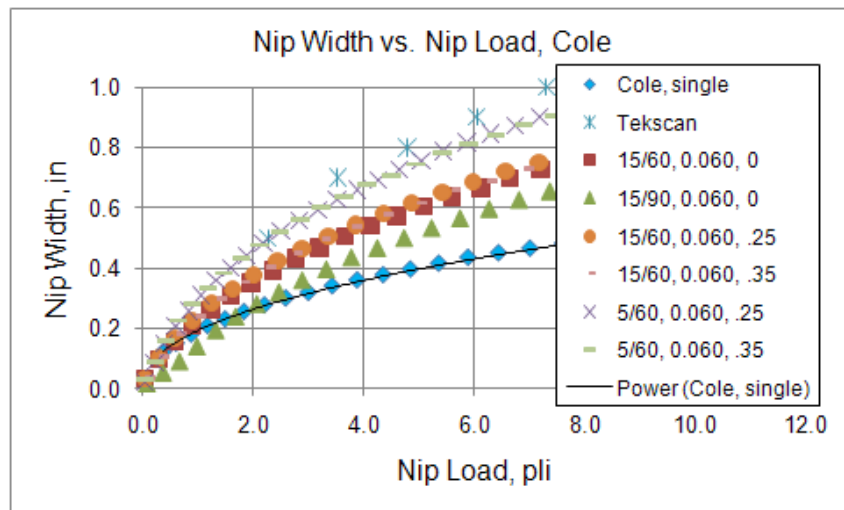


Figure 8: Nip width versus nip load, single/dual durometer nip rollers

durometer = unknown, inner layer Poisson's ratio unknown, outer layer durometer = 60 Shore A, outer layer Poisson's ratio assumed equal to 0.46). Figures 8 and 9 show the theoretical and experimental nip width versus nip load and creep versus nip load for the dual durometer roller and the theoretical results only for the single durometer roller. Correlation between the model and experiment required some iteration on the hardness and Poisson's ratio of the lower layer on

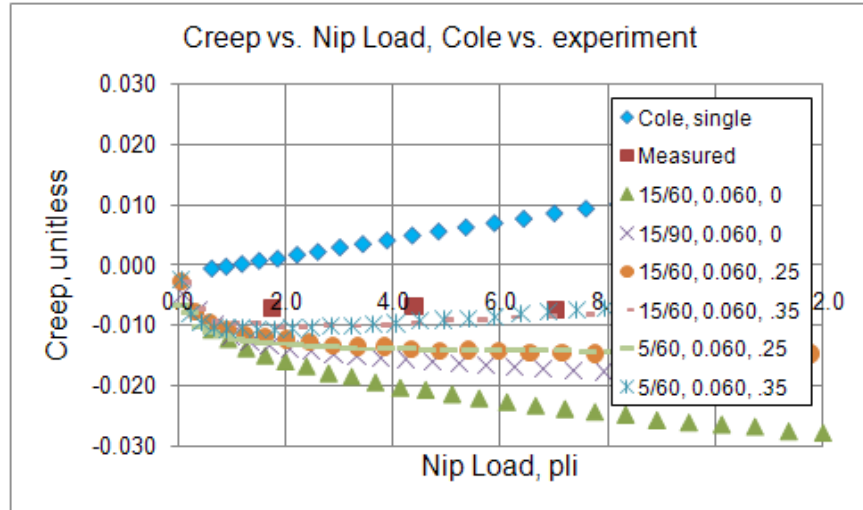


Figure 9: Creep versus nip load, single/dual durometer nip rollers

the dual durometer roller. A value of durometer equal to 5 Shore A and a Poisson's ratio of 0.35 gave the best agreement between the model and predicted results. Interestingly, the dual durometer roller had negative creep indicating that the roller actually traveled faster in the test module during the experiments.

### Width Dependent Nip Roller Feed Rate

Roller deflection due to end-loaded nip rollers leads to width-dependent deflection, nip width, and nip roller feed rate. This behavior is analyzed using Euler beam bending theory where the roller shell is modeled as a beam. Deflections arise from nonuniform distributed loads arising from the compression of the elastomeric cover due to end loads applied through the mounting bearings. Figure 7 shows the geometry of this system. A model was developed to predict the response of this system accounting for the slightly nonlinear behavior of the cover load versus deflection behavior indicated in Figure 4. Results from this model are presented for the baseline nip roller pair for which results were presented in Figures 4 through 6. Figure 10 shows roller deflection and Figure 11 shows nip load, nip width, creep and max centerline stress versus width position. Experimentally measured nip width and max centerline stress are also indicated in the graphs. Observation of the results indicates very good agreement between the predicted and measured nip widths. The max centerline stress is not quite as accurate but does show the correct trends.

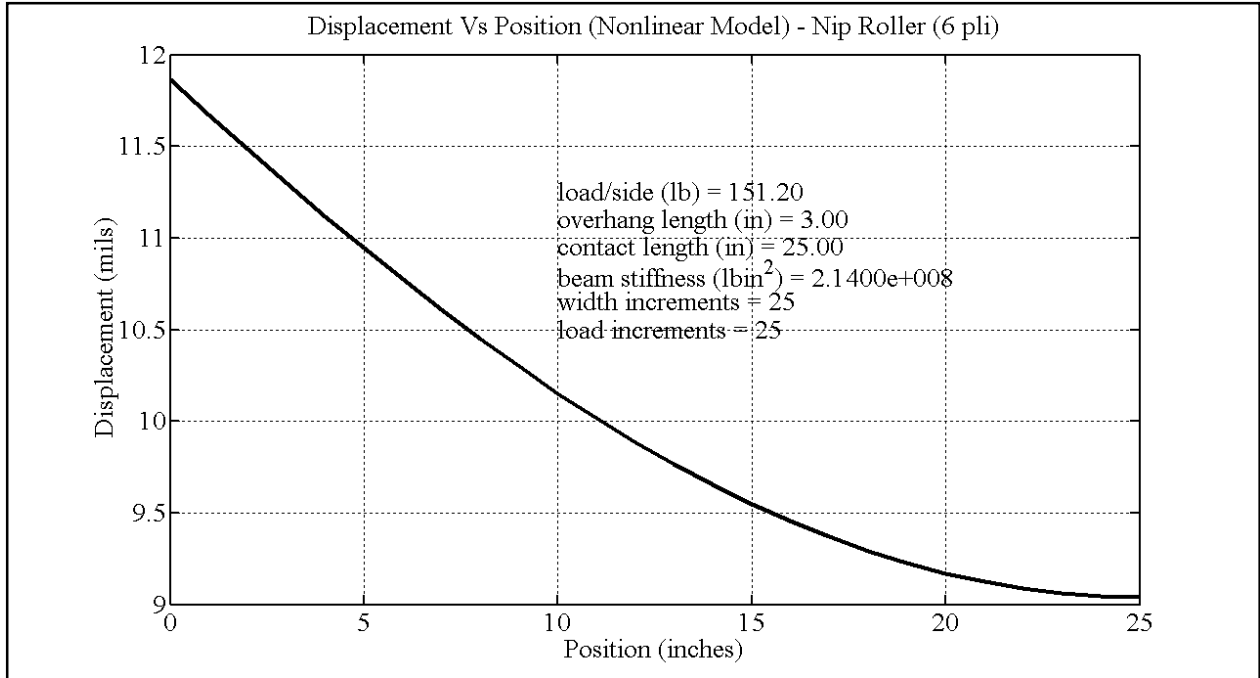


Figure 10: Roller Deflection versus Width Position, baseline case

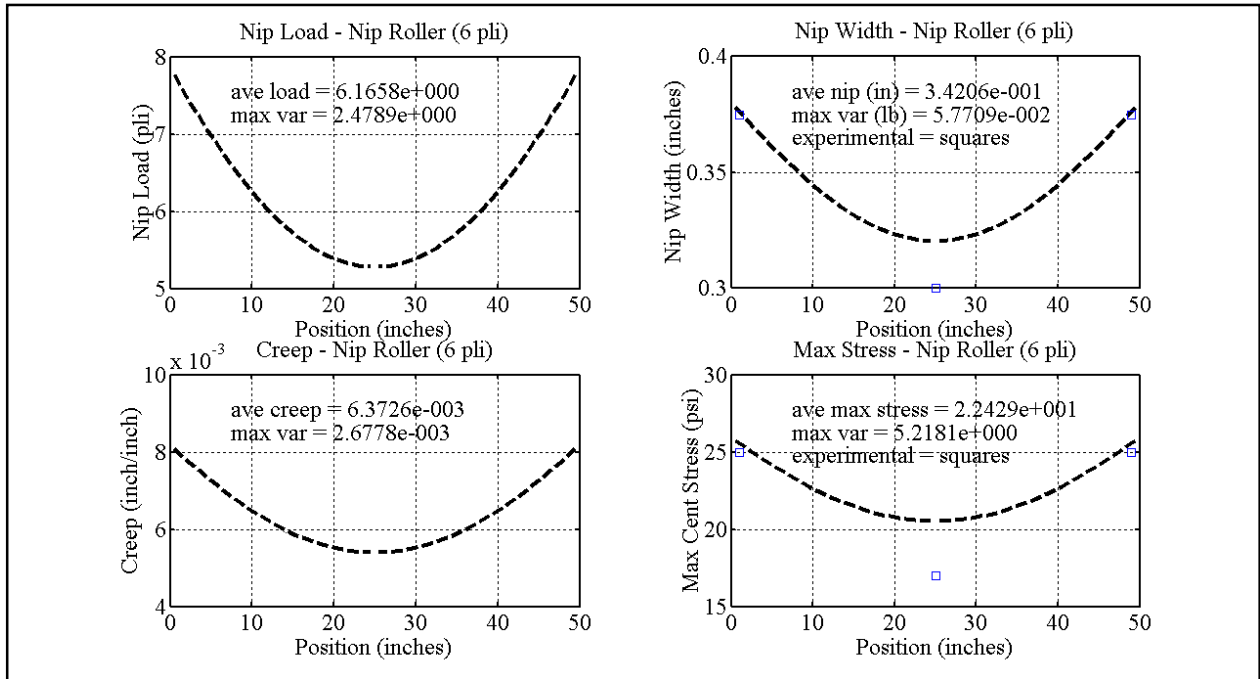


Figure 11: Nip Load, Width, Creep, Peak Pressure versus Width Position, baseline case

Figures 12 and 13 show the very interesting comparison to the dual durometer roller for which results were presented in Figure 8 and 9. Observation of these results indicates several things. First, the variation in nip load across the width is comparable to the baseline case. Second, the nip width variation is significantly smaller for the dual durometer roller while the average nip

width is significantly larger. This is due to the significantly reduced stiffness of the dual durometer covering. This leads to the third observation that the max centerline stress is much lower for the dual durometer roller.

Finally, and most importantly for the purposes of this paper, are the observations related to creep. Here, we see that the average creep for the dual durometer roller is comparable in size but negative compared to the baseline case. This means that the roller is rotating at a faster speed compared to the idling backup roller. By judicious selection of the cover characteristics, the average creep for the dual durometer roller could be designed to be equal to zero.

Of even greater interest is the comparison between the variation in creep across the width between the baseline case and the dual durometer case. Here, the variation in creep is more than an order of magnitude smaller for the dual durometer roller ( $1.75e-4$ ) compared to the baseline case ( $2.68e-3$ ). This is extremely beneficial in that the dual durometer roller will be significantly less sensitive during the conveyance of webs due to end-to-end loading variations and roller axial misalignment. In addition, the creep behavior of the dual durometer roller will desensitize its response to localized variations in roller deflection (e.g., that might arise from web gauge variability).

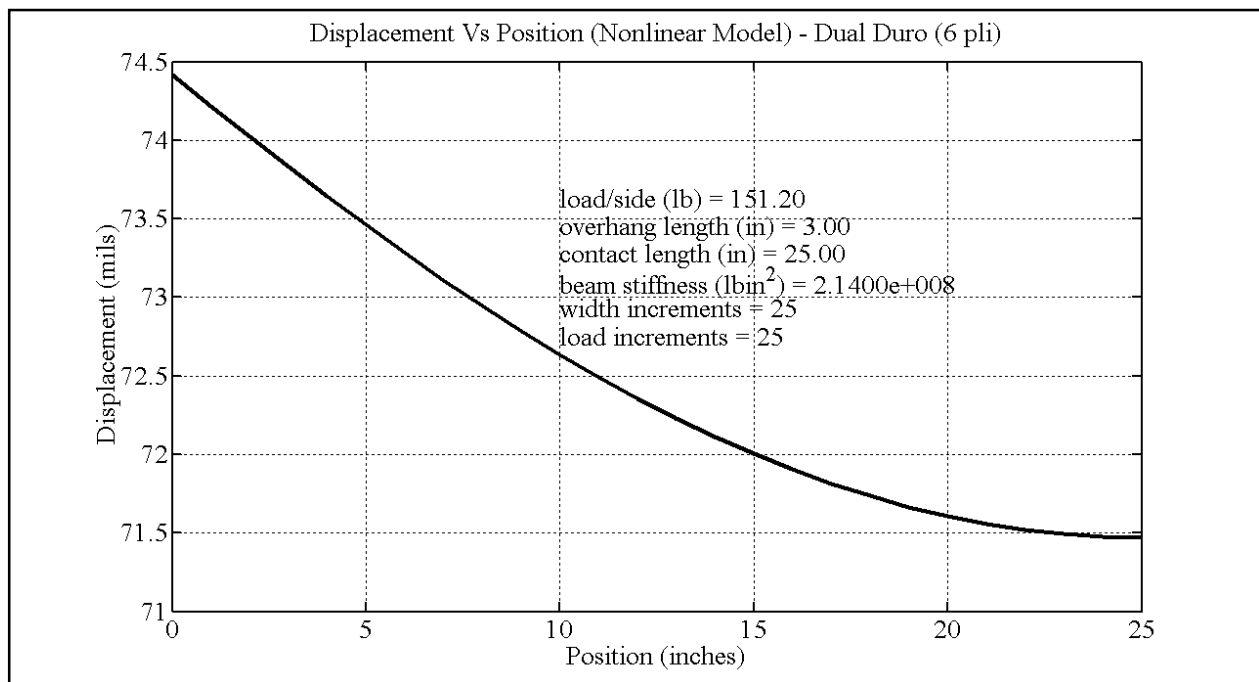


Figure 12: Roller Deflection versus Width Position, dual durometer

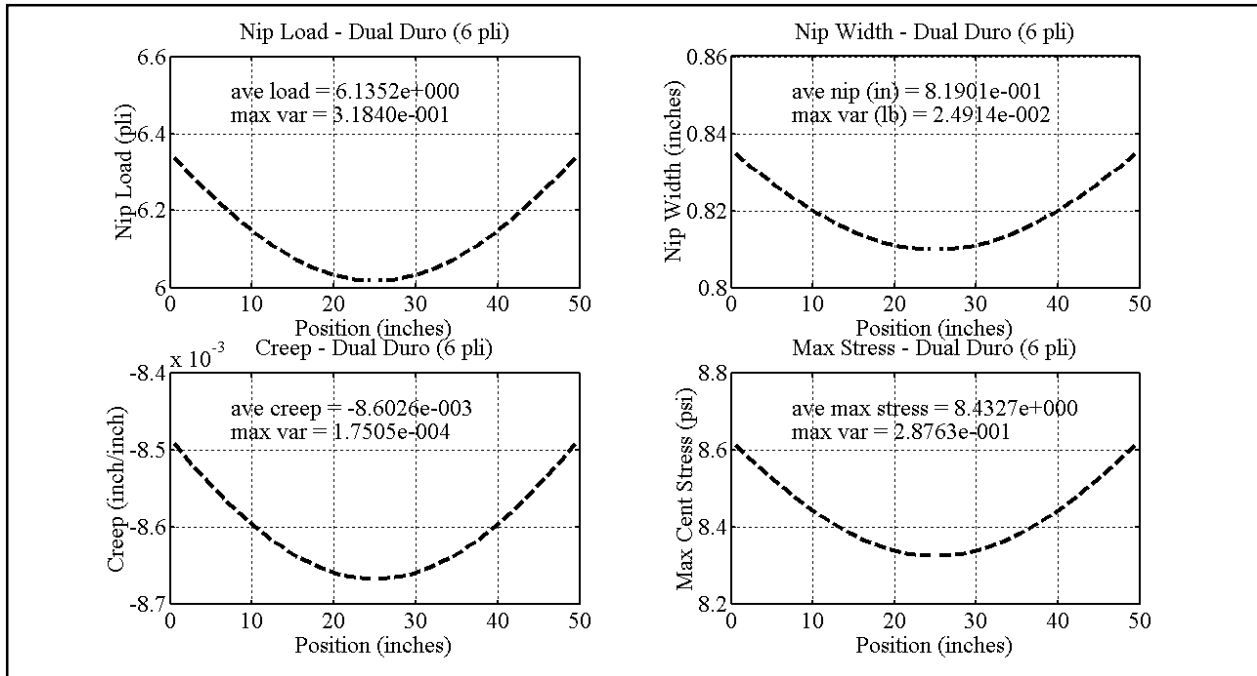


Figure 13: Nip Load, Width, Creep, Peak Pressure versus Width Position, dual durometer

## Conclusions

Two theoretical models predicting creep within a nip roller pair consisting of a uncovered roller nipped against an elastomeric covered roller have been presented. A method for collecting experimental creep data has also been described. Experiments were conducted to collect data to compare to the theoretical models. Results for both a single durometer cover and a dual durometer cover were obtained and compared to model predictions where appropriate. Good agreement between the models and experiments was demonstrated. A model was also presented to predict creep across the width in a nipped roller system and results shown for baseline (single durometer) and a dual durometer cases. Results indicate that the dual durometer roller will be a superior performer in terms of variation in creep across the width and therefore will be much more robust to end loading and alignment variability.

## Acknowledgements:

The author thanks American Roller Company for their contribution of the single and dual durometer pressure roller covering and Tim Walker and Mike Kubiak for their assistance with data collection and analysis.

## References:

1. Stack, K.D., et. al, "The Effects of Nip Parameters on Media Transport", Proceedings of the 3<sup>rd</sup> International Conference on Web Handling, Stillwater, OK, 1995, ed J K Good, pp 382-395.

2. Good, J.K, "Modeling Rubber Covered Nip Rollers in Web Lines", Proceedings of the 6<sup>th</sup> International Conference on Web Handling, Stillwater, OK, 2001, ed J K Good, pp 159-177.
3. Cole, K.A., "Measurement and Modeling of Nip Roller Feed Rates", Proceedings of the 2<sup>nd</sup> Applied Web Handling Conference, Rochester, NY, 2010.
4. Cole, K.A., "Roller Overdrive Analysis", Eastman Kodak Internal Publication, April 21, 1983.
5. Hannah, M., Quart. J. Mech. Appl. Math., Vol. 4, p. 94, 1951.
6. Parish, G.J., "Calculation of the Behaviour of Rubber-Covered Pressure Rollers", British J. of App. Physics, Vol. 12, p. 333, July 1961.
7. Timoshenko, "Theory of Elasticity", McGraw-Hill Book Company, Third Edition, pp 53-60.

Author Contact Information:

Dr. Kevin Cole

Senior Web Handling Development Engineer

Optimation Technology Incorporated

Rochester, New York 14652-3254

585-703-0514 (work phone), 585-321-2700 (fax)

e-mail: kevin.cole@optimation.us